Cellulose (2021) 28:7355–7372
https://doi.org/10.1007/s10570-021-03975-8

ORIGINAL RESEARCH

Synthesis of an effective halogen-free flame retardant rich in phosphorus and nitrogen for lyocell fabric

Yingbin Guo · Mengyuan Xiao · Yuanlin Ren · Yansong Liu · Yang Wang · Xun Guo · Xiaohui Liu

Received: 25 November 2020 / Accepted: 25 May 2021 / Published online: 29 May 2021

Abstract A novel effective halogen-free flame retardant (FR) rich in phosphorus (P) and nitrogen (N) was synthesized via Mannich and esterification reaction of ethanolamine, glyoxal, phosphoric acid and urea, and used for the preparation of durable flame retardant lyocell fabric (FR-lyocell). Its chemical structure was characterized by Fourier transform infrared spectra, ^{1}H and ^{31}P nuclear magnetic resonance spectra. Inductively coupled plasma emission spectrometry and elemental analysis were conducted to test the phosphorous, carbon and nitrogen contents. The results confirmed that the FR was successfully synthesized and grafted on the lyocell fabric via firm P–O–C covalent bonds. The limiting oxygen index of the FR-lyocell treated with 30 wt% flame retardant finishing solution is 44.6%, demonstrating high efficiency flame retardancy. The thermo-gravimetric analysis indicated that FR-lyocell degraded preferentially than that of the control sample and the char residue was 38.8 wt% at 800 °C in N_2 atmosphere. In addition, the cone calorimeter test revealed that FR-lyocell could not be ignited and the peak of heat release rate was much lower than that of original specimen. Furthermore, the char residue of FR-lyocell is compact and the I_D/I_G value is 0.771, exhibiting a super degree of carbonization. Moreover, TG-IR result revealed that FR played dual flame-retardant effect in the gaseous and condensed phases. The flame retardant finishing has a negligible impact on the mechanical properties of the fibers. In summary, FR-lyocell exhibits excellent flame retardancy and superior char forming capability, which is suitable for the preparation of flame retardant lyocell fibers.

Y. Guo · M. Xiao · Y. Ren (✉) · Y. Liu · Y. Wang · X. Guo
School of Textile Science and Engineering, Tiangong University, Tianjin 300387, China
e-mail: yuanlinr@163.com

Y. Ren
Key Laboratory of Advanced Textile Composite, Ministry of Education, Tiangong University, Tianjin 300387, China

X. Liu (✉)
School of Materials Science and Engineering, Tiangong University, Tianjin 300387, China
e-mail: xiaohuilau@163.com

Graphic abstract

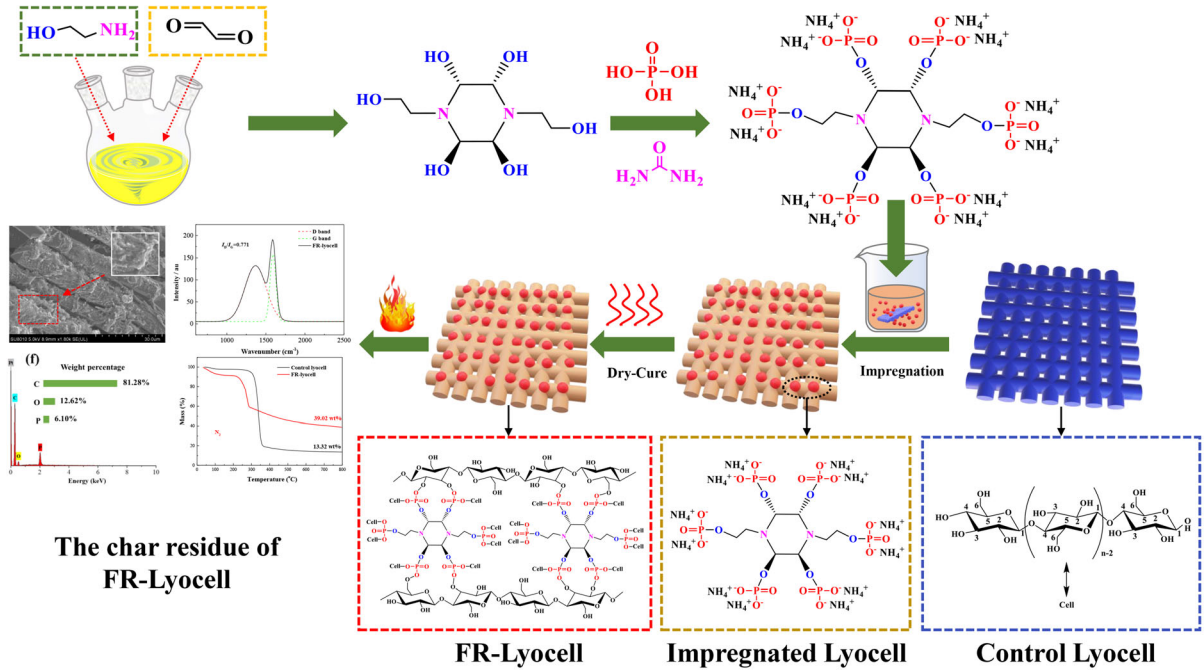

Keywords Flame retardant · Nitrogen and phosphorus · Lyocell fibers · Mechanism · Properties

Introduction

Lyocell fiber is a kind of green, environmental and regenerable cellulose fibers (Joshi et al. 2010). It possesses various excellent properties, such as non-toxicity, biodegradability, comfortable and softness (Shibata et al. 2004). However, the limiting oxygen index (LOI) of lyocell fiber is only 18.0% and it is extremely easy to be ignited and burned (Dong et al. 2017; Li et al. 2010). The flammability of lyocell fiber or its fabric severely restricts its application. Thus, it is essential to improve the flame retardancy of lyocell fiber and its fabric (Xie et al. 2013).

Up to now, various strategies have been developed to enhance the flame retardancy of lyocell fiber or fabric, which mainly include blend spinning (Seddon et al. 1996), finishing process (Alongi et al. 2011b; Mengal et al. 2016; Liu et al. 2018a, b; Li et al. 2020a), and chemical treatment (Bai et al. 2014; Wang et al. 2016; Liang et al. 2017; Cheng et al. 2017). For example, Seddon et al. blended *N*-hydroxymethyl-3-(dimethoxyphosphonyl) propionamide (Pyrovatex CP) with cellulose spinning solution and prepared excellent flame retardant lyocell fiber by wet-spinning technique (Seddon et al. 1996). The LOI value of the resulted fiber with 32.0 wt% addition of Provatex CP is 40%. For blend spinning scenario, the particle size of flame retardant, the compatibility between flame retardant and spinning solution, and the migration of flame retardant should be focused on. Additionally, a relatively large amount of flame retardant is added to achieve good flame resistance, which, as a result, will deteriorate the mechanical properties of the resulted fiber (Grancaric et al. 2015). The finishing process, such as dipping, padding, curing, coating (Wang et al. 2020), spraying, etc., is another common technique for the preparation of flame retardant cellulose fibers. The fibers or fabrics were finished through a multi-component system which commonly contained flame retardants, cross-linking agents, and curing agents so as to ensure flame retardancy (Alongi et al. 2011b). Provatex CP was also used to treat lyocell fibers with citric acid as a cross-linker via finishing process

(Mengal et al. 2016). The char residue of the treated lyocell fibers was 42.0 wt%, implying high char-forming ability. However, the introduction of cross-linking agents has a negative effect on fibers and worsens the flame retardancy of the treated samples. Conversely, chemical treatment is an effective and durable strategy to achieve the desired flame retardancy by forming firm covalent bonds between fibers and flame retardant (Bai et al. 2014; Jia et al. 2017; Chen et al. 2013). Recently, phosphorous-containing flame retardants with reactive functional groups $–P=O(NH_4)_2$ have been used for preparation of flame retardant cotton (Jia et al. 2017; Gao et al. 2015; Zhang et al. 2020). Recently, a bio-based phosphorus and nitrogen-containing ammonium salt flame retardant was synthesized and used for the highly efficient preparation of durable flame retardant cellulose fabric (Wan et al. 2019a; Ren et al. 2020; Liu et al. 2020). A plant-based non-formaldehyde and high phosphorus-containing ammonium phytate (APA) flame retardant was synthesized for cotton fabric (Feng et al. 2017). The modified cotton fabric exhibited improved flame retardancy and durability. These effective flame retardants have significant potential in practical application. So far, to develop efficient, non-toxic, and eco-friendly flame retardants, phosphorus-containing compounds are often used as alternatives for halogen-containing compounds and have synergistic effects with nitrogen-containing compounds (Bai et al. 2014; Jia et al. 2017). These works demonstrated that ammonium salts could be grafted on the surface of cellulose fibers via the firm P–O–C covalent bonds through the classical dip-dry-cure technique and the flame retardancy of cellulose fibers was obviously improved (Xu et al. 2018; Liu et al. 2019; Ren et al. 2020). The lyocell fabric treated with phosphorus-containing and nitrogen-containing flame retardant possessed good durability, low fuel volatility, low pyrolysis temperature, and excellent char formation ability during combustion (Naik et al. 2015). Ethanolamine is a highly reactive substance owing to the $–NH_2$ and –OH groups. The $–NH_2$ groups can react with the aldehyde via Mannich reaction (Peng et al. 2020; Kazantsev et al. 2020), while the –OH can undergo the esterification reaction with organic or inorganic acid (Tian et al. 2019; Jia et al. 2017). Therefore, in this work, a novel effective halogen-free flame retardant rich in phosphorus and nitrogen was synthesized via Mannich and esterification reaction using low-cost materials, such as ethanolamine, glyoxal, phosphoric acid, and urea. Subsequently, the highly efficient and durable flame retardant lyocell fabric (FR-lyocell) was prepared through the classical dip-dry-cure technique. Then, the flame retardancy, thermal properties, structure of the char residue, and combustion performance were confirmed by limiting oxygen index (LOI), thermogravimetric analysis (TGA), scanning electron microscope (SEM), combustion testing, and cone calorimeter testing. Finally, the flame retardant mechanism of FR-lyocell during combustion was investigated by thermogravimetry-infrared spectroscopy (TG-IR) and Raman spectroscopy.

Experimental section

Materials

Lyocell fabrics (plain weave with the basic weight of 150 g/m^2) were obtained from Tiangong University (Tianjin, China). Ethanolamine (99%) was purchased from Aladdin Chemistry Industry Co. Ltd. (Shanghai, China). Glyoxal (40%), urea, phosphoric acid (H_3PO_4, 85%) and absolute alcohol were obtained from Tianjin Kemiou Chemical Reagent Co., Ltd. (Tianjin, China). Dicyandiamide was purchased from Nanjing Xiezun Chemical Agent Co. Ltd. (Nanjing, China). All reagents were analytical reagent grade and used without further purification.

Synthesis of flame retardant (FR)

Ethanolamine (6.17 g, 0.1 mol), glyoxal (14.51 g, 0.1 mol), H_3PO_4 (69.18 g, 0.6 mol), and 20 mL of deionized water were mixed in a 250 mL three-neck bound flask equipped with allihn condenser. The reaction mixture was then heated at 170 °C for 5 h by using an oil bath. Afterwards, urea (36.04 g, 0.6 mol) was added into the mixture, heated at 160 °C for about 1.5 h. The crude product was then precipited with absolute ethanol to obtain a solid brown product with an 85.84% yield. The synthesis route of the FR is shown in Scheme1.

Fabrication of flame retardant lyocell (FR-lyocell)

The flame retardant (FR) was dissolved in a specific amount of deionized water to obtain 20, 30, and

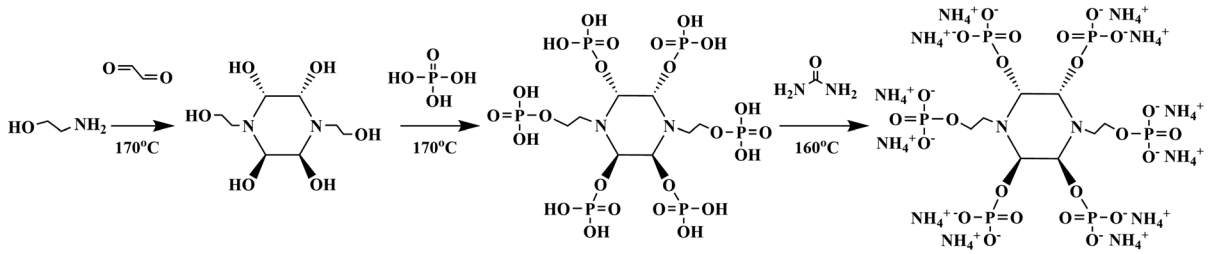

Scheme 1 Synthesis of the flame retardant

40 wt% flame retardant finishing solution, respectively. In addition, 6 wt% dicyandiamide as a catalyst was added into the solution. The lyocell samples were preliminarily washed with deionized water and absolute ethanol mixture solution several times and dried. Then, they were soaked in the flame retardant solution with a bath ratio of 1:30 (fabric weight: volume of the solution) at 70 °C for 3 h. After that, the impregnated specimens were taken out and squeezed gently to make the liquid retention maintain at about 120 wt%. Finally, the samples were dried at 120 °C for 6 min, followed by baking at 180 °C for 3 min. The treated samples were washed with running water and then dried at 60 °C in an oven to a constant weight. The flame retardant lyocell (FR-lyocell) was then obtained. The reaction of FR and lyocell samples is shown in Scheme 2. The weight gain (*WG*) of the treated lyocell sample is calculated by the following Eq. (1):

$$WG = [(m_2 - m_1)/m_1] \times 100\% \quad (1)$$

where m_1 and m_2 are the weights of the control and treated samples, respectively.

In this study, the treated fabrics with a *WG* of 14.14 wt% were selected for the subsequent experiments.

Characterization

1. The structure of the FR was characterized by ^{1}H NMR and ^{31}P NMR using a Bruker AV III 600 spectrometer (Bruker Corporation, Billerica, MA, USA). Deuterium oxide (D_2O) was used as a solvent and tetramethylsilane (TMS) was used as an internal standard.
2. The LOI of lyocell fabrics were tested using a digital display oxygen index apparatus (M606B, Qingdao Shanfang Instrument Co. Ltd., Qingdao, China) in accordance with the standard of ASTM D2863-2000. The flame retardant durability of the modified fabrics with the size of 50 mm × 100 mm was washed according to AATCC 61-2003 test No. 1A with 0.37 wt% detergent. One laundering cycles (LCs) lasting for 45 min equals five commercial launderings.

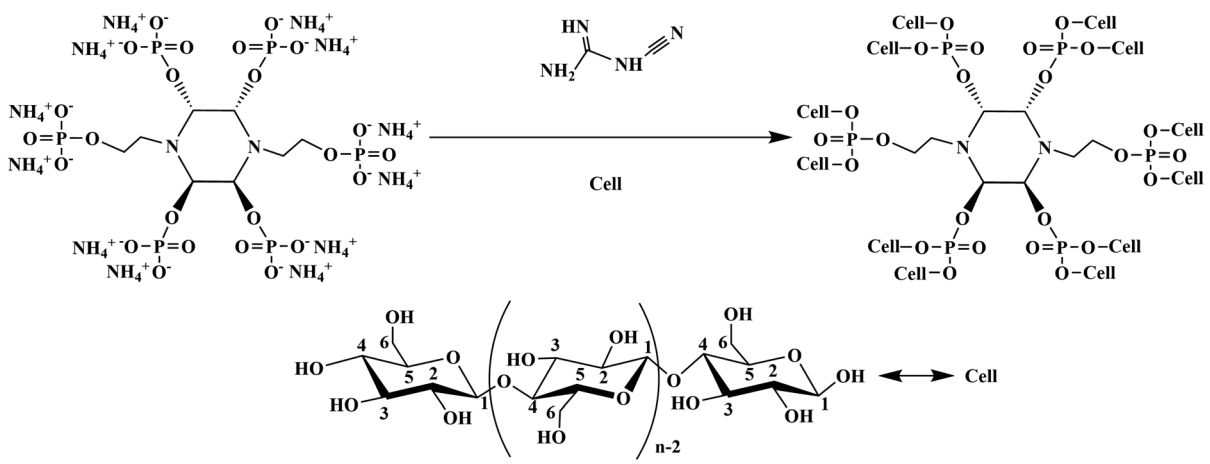

Scheme 2 Preparation of the flame retardant lyocell

In addition, the flame retardancy of the treated lyocell fabrics after different laundering cycles with the size of 50 mm × 100 mm × 1.0 mm were performed by simple burning testing. To access the fastness of flame retardant, the control and FR-lyocell were conducted wet rubbing by Y571 dying rubbing fastness tester (Laizhou Yuanmao Instrument Co. Ltd, China) according to GB/T 3920-2008. Then, the LOI values of treated specimens were tested.

3. X-ray photoelectron spectroscopy (XPS) of the control and the treated lyocell fabric was obtained on a K-alpha model (American THERMOFISHER Company) with the power of 150 W, beam spot at 400 μm and energy analyzer fixed at 50 eV.
4. Inductively coupled plasma emission spectrometry (ICP) was conducted with an ICPS-5110 (Aglient, America) instrument to test the phosphorous contents in FR and FR-lyocell. Elemental analysis (EA) of FR and FR-lyocell was tested with a Euro EA 3000 series elemental analyzer (Leeman Labs Inc., USA) to get the carbon and nitrogen contents.
5. The FTIR spectra of FR, control lyocell, FR-lyocell, and FR-lyocell (30 LCs) were recorded on Nicolette iS50 FTIR spectrophotometer (Thermo Fisher Scientific Inc., China.) with KBr pellets pressing method. The wavelength ranged from 4000 to 500 cm^{-1}, and the resolution was 2.0 cm^{-1}.
6. The crystalline structures of the lyocell and treated lyocell fabric were tested by X-ray diffraction (XRD) (Beijing Purkinje General Instrument Co., Ltd., Beijing, China). The diffraction angle ranged from 2° to 52° with a step size of 0.2° (λ = 0.154 nm).
7. Thermogravimetric analysis (TGA) was performed on a STA449F3 (Germany NETZSCH Company) thermogravimetric analyzer ranging from 35 to 800 °C, with a heating rate of 10 °C/min under nitrogen and air atmosphere, respectively.
8. The combustion behaviors of the control and treated lyocell fabric with the size of 100 mm × 100 mm × 1.0 mm were carried out on an FTT0006 cone calorimeter instrument (FTT, United Kingdom) under the radiation power of 35 kW/m^2. The heat release rate (HRR), the peak of heat release rate (PHRR), total heat release (THR), time to ignition (TTI) were measured. In addition, the ratio of PHRR and time to PHRR, i.e., the fire growth rate index (FIGRA), was calculated.
9. Thermogravimetric analysis coupled with Fourier transform infrared analysis (TG-FTIR) was conducted on an STA 6000 Frontier TGA (Perkin Elmer, Waltham, MA, USA) coupled with a Nicolet FTIR (Thermo Fisher Science, Waltham, MA, USA). The decomposed compounds of the FR-lyocell samples were transferred from TGA analyzer to the TG-FTIR interface via a stainless transfer pipe. The testing was carried out with a nitrogen flow at a rate of 50 mL/min and the temperature ranged from 25 to 800 °C with a heating rate of 10 °C / min. The released gases were characterized by an FTIR spectrometer ranging from 500 to 4000 cm^{-1} with a resolution of 2 cm^{-1}.
10. Laser Raman instrument (XploRA PLUS, Horiba, Japan) was employed to characterize the graphitization degree of the residual char in the range of 500–2500 cm^{-1}.
11. The surface of the lyocell fabric was observed by scanning electron microscopy (SEM) with energy dispersive spectroscopy (EDS) (Hitachi S-4800, Hitachi Corp., Tokyo, Japan). The fabric was gold-plated before testing. The test voltage was 10 kV with a working distance of 6–8 mm, and the magnifications were 800 and 2000, respectively.
12. The tensile strength and breaking elongation of the control and FR-lyocell fabrics were measured on INSTRON-3369 strength tester (Instron Co. Ltd., America) according to GB/T 3923.1-1997 method. The size of specimens is 150 mm × 50 mm × 1.0 mm. The gauge length is 100 mm and the stretching speed is 100 mm/min. Each group of samples is tested five times and the average value is calculated to reduce the error.

Results and discussion

NMR analysis of FR

The molecular structure of FR was characterized by hydrogen-1 nuclear magnetic resonance (^{1}H NMR), and phosphorus-31 NMR (^{31}P NMR) spectroscopy. Figure 1a shows the ^{1}H NMR spectra of FR. The peak at 4.67 ppm is assigned to hydrogen atoms in D_2O (s, deuterium oxide). The peak at 1.03–1.04 ppm attributes to hydrogen atoms (t, C_1, $2H_2$) in N–CH_2 (a). The peak at 3.51–3.52 ppm corresponds to hydrogen atoms (t, C_2, $2H_2$) in O–CH_2 (b). The peak at 4.77 ppm is ascribed to hydrogen atoms (s, C_3, 4H) in C–H (c). In addition, the peak at 7.07 ppm belongs to hydrogen atoms of NH_4^+. Meanwhile, the integra areas ratio of a:b:c is 0.86:0.78:0.84 in the spectra, which is accorded with the number ratio of corresponding hydrogen protons in FR. For ^{31}P NMR spectra, the peaks at 0.00 and 0.69 ppm are owing to the phosphorus atoms of the FR.

LOI values and weight gain

The limiting oxygen index (LOI) test is commonly used to evaluate the flame retardancy of materials. The weight gains (*WGs*) and LOI values of the lyocell fabrics treated with different FR concentrations and several laundering cycles (LCs) are listed in Table 1. The LOI value of the control lyocell is only 18.0%. The *WG*s of the lyocell fabric treated with 20 wt%, 30 wt% and 40 wt% FR is 10.03 wt%, 14.14 wt%, and 15.57 wt%, respectively. This indicates that with the increase of the concentration of FR solution, the *WG*s gradually increase accordingly. Besides, the LOI values of the treated lyocell fabrics with 20 wt%, 30 wt%, and 40 wt% FR are 34.8%, 40.6% and 44.2%, respectively, which are much higher than that of the control sample. With the increase of LCs, the LOI values of FR-lyocell gradually decrease. This may be caused by the gradually abrasion of fibers resulting in removing of the adsorbed FR on the surface of lyocell fibers. Meanwhile, the LOI value of the sample treated with 20 wt% FR is 25.7% after 30 LCs, which can be considered as a semidurable flame retardant fabric. Moreover, the LOI values of the FR-lyocell treated with 30 wt% and 40 wt% FR finishing solution retained 31.3% and 33.7% after 30 LCs, which can be considered durable flame retardant lyocell fabric (Lu et al. 2018a). In addition, the LOI values of the samples treated with 20 wt%, 30 wt% and 40 wt% FR is 30.6%, 35.6% and 40.7% after wet rubbing. These results demonstrate that the FR prepared in this work endows lyocell fabric with excellent flame retardancy and durability.

Flammability

To further research the flame retardancy and washability of the lyocell fabrics, simple burning testing was performed for the blank and treated lyocell specimens after different LCs and lyocell fabrics treated with 30 wt% FR solution after web rubing as shown in Fig. 2. The lyocell fabric is almost burnt out. Compared to the control sample, all the FR-lyocell fabrics could not be ignited under a vertical flame and almost

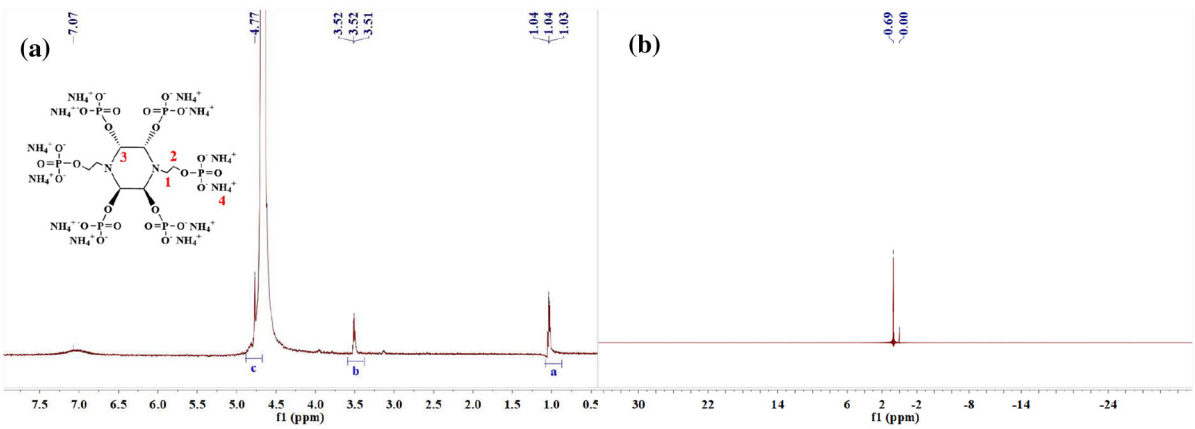

Fig. 1 ^{1}H NMR (**a**) and ^{31}P NMR (**b**) spectra of FR

Table 1 The LOI and *WG* values of lyocell fabric treated with different FR concentrations before and after different laundering cycles (LCs), and after wet rubbing

FR concentration (wt%)	*WG* (wt%)	LOI (%)				
		0 LCs	10 LCs	20 LCs	30 LCs	After wet rubbing
0	0	18.0	–	–	–	–
20	10.03	34.8	31.0	27.7	25.7	30.6
30	14.14	40.6	36.7	34.3	31.3	35.6
40	15.57	44.2	42.9	38.8	33.7	40.7

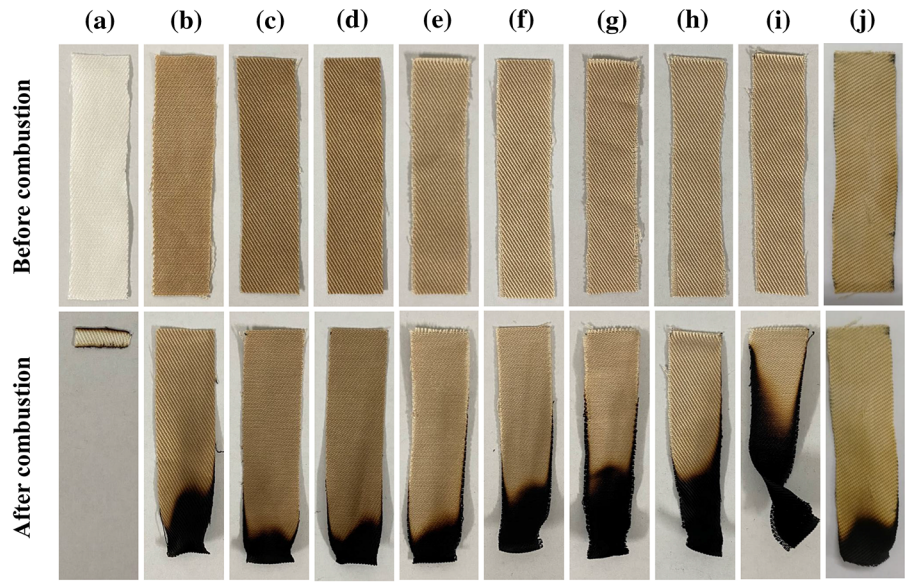

Fig. 2 Photos of the different fabrics before and after vertical burning: control sample (**a**); lyocell fabrics treated with 20 wt% (**b**), 30 wt% (**c**) and 40 wt% (**d**) FR solution; lyocell fabrics treated with 30 wt% FR solution after 10 LCs (**e**), 20 LCs (**f**), 30 LCs (**g**), 40 LCs (**h**), 50 LCs (**i**) and after wet rubbing (**j**)

maintained the original shape due to the formation of a complete and continuous protective char frame. Furthermore, the flame retardancy of the fabric becomes better with the increase of FR concentration. Additionally, with the increase of laundering cycles (LCs), the burning becomes relatively easy and the char residue of the sample is slightly distorted after 50 LCs. This phenomenon was ascribed to the presence of phosphoric acid groups in FR, which effectively enhanced the char-forming ability of FR-lyocell (Dong et al. 2017; Bai et al. 2014). In addition, the nitrogen element could generate ammonia (NH_3) during combustion, which diluted the flammable gases. Morover, lyocell fabrics treated with 30 wt% FR solution after web rubing still able to self-extinguish. These results indicated that the FR prepared in this work endows lyocell fabric with good washing durability and superior char-forming capability.

XPS analysis

The surface chemical composition of the pristine, FR-lyocell and FR-lyocell (30 LCs) samples were investigated by XPS, as shown in Fig. 3. For the pristine fabric, the strong peaks at 286 eV and 533 eV correspond to carbon (C) and oxygen (O) atoms (Liu et al. 2020; Zhang et al. 2020) with the content of 64.49 at.% and 30.58 at.%, respectively. For the FR-lyocell, two new peaks at 400 eV and 134 eV are

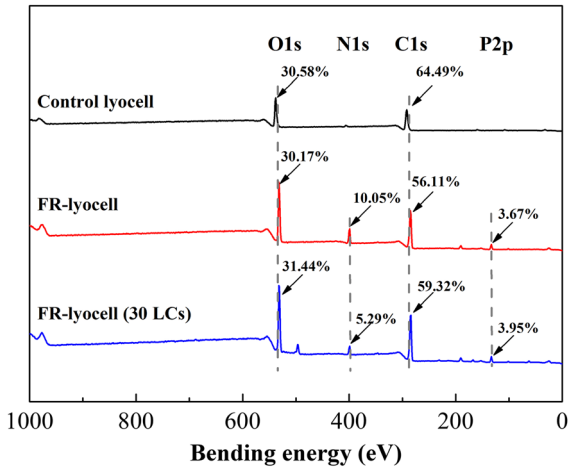

Fig. 3 XPS spectra of control lyocell, FR-lyocell, and FR-lyocell (30 LCs)

attributed to nitrogen (N) and phosphorus (P) components, respectively. And the content of C, O, N, and P elements is 56.11 at.%, 30.17 at.%, 10.05 at.%, and 3.67 at.%, respectively. This indicates that FR has been successfully grafted on the lyocell fiber surface. In addition, for the FR-lyocell fabric (30 LCs), there are the same peaks as FR-lyocell. And the content of C, O, N, and P elements are 59.32 at.%, 31.44 at.%, 5.29 at.%, and 3.95 at.%, respectively. The slight difference in chemical composition between FR-lyocell and FR-lyocell fabric (30 LCs) is due to the removal of trace amount of flame retardant adsorbed on the fiber surface caused by mechanical friction. The result reveals that the FR-lyocell possesses better washing resistance.

ICP and EA analysis

Since phosphorous (P) and nitrogen (N) elements are the main components conferring fire properties to materials, determination of the P and N contents in FR and FR-lyocell was performed. The results of elemental analysis (EA) and P contents tested by ICP are listed in Table 2. As shown in Table 2, the P contents in FR and FR-lyocell are 24.34 wt% and 2.27 wt%, respectively, which indicates that the FR contains higher P elements and P element is introduced into cellulose after flame retardant finishing. On the other hand, the N contents in FR and FR-lyocell is 12.10 wt% and 2.72 wt%. It is important to note that the N element in FR come from the C–N group and ammonium ion (NH_4^+). However, the N element in FR-lyocell mainly comes from the C–N group after flame retardant finishing. According to the above tests and analysis, it can be confirmed that the FR rich in P and N elements was successfully grafted onto the lyocell fabric. This is consistent with the XPS test results.

Table 2 EA and ICP of FR and FR-lyocell analysis

Sample	C (wt%)	N (wt%)	P (wt%)
FR	0.41	12.10	24.32
FR-lyocell	38.18	2.72	2.27

FTIR infrared and X-ray diffraction

The FTIR spectra of FR, control lyocell, FR-lyocell, and FR-lyocell (30 LCs) samples are shown in Fig. 4. All FTIR spectra show strong peaks at 3320 cm^{-1} and 2890 cm^{-1}, respectively, which are assigned to the stretching vibration absorption of –OH (Sahito et al. 2015; Xu et al. 2017) and C–H (Wei et al. 2018; Wan et al. 2019b). The characteristic absorption peaks of FR at 1402 cm^{-1}, 1262 cm^{-1}, 1080 cm^{-1} and 845 cm^{-1} are attributed to the absorption of C–N bond (Yang et al. 2018), P=O group (Liu et al. 2020; Wang et al. 2016), P–O–C bond (Tian et al. 2019; Wan et al. 2019a) and P–OH group. These results confirm the successful synthesis of FR. Besides, both of the

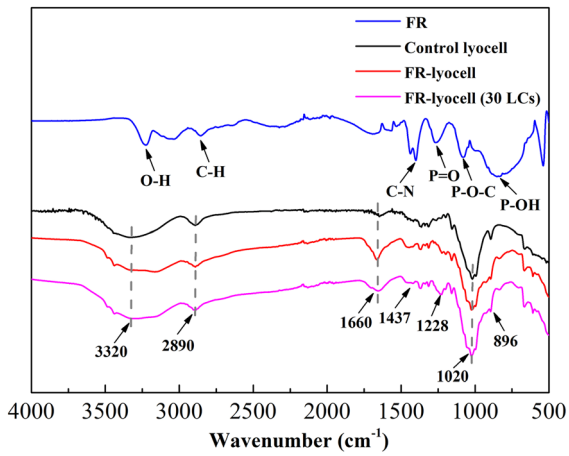

Fig. 4 FTIR spectra of FR, control lyocell, FR-lyocell and FR-lyocell (30 LCs)

control lyocell and FR-lyocell show weak peak at 1660 cm^{-1}, which is attributed to the stretching vibrations of C=O bond (Wang et al. 2016; Wan et al. 2019a). Moreover, four new characteristic absorption peaks of FR-lyocell are observed at 1437 cm^{-1}, 1228 cm^{-1}, 1020 cm^{-1} and 896 cm^{-1} attributing to the absorption of C–N bond, P=O group, P–O–C bond and P–OH bond, respectively. However, these characteristic peaks do not occur at the spectrum of control lyocell sample, indicating the reaction of FR with –OH of lyocell fibers and forming the P–O–C covalent bond. For the FR-lyocell (30 LCs), there are the same peaks as FR-lyocell, indicating good washing resistance of FR-lyocell sample. The FTIR result is consistent with the XPS analysis, which fully proves that the FR has been synthesized and successfully grafted onto the surface of lyocell fibers via P–O–C covalent bond.

Figure 5 shows the X-ray diffraction pattern of the control and FR-lyocell sample. The diffraction peaks at 12.32°, 20.26°, 21.89°, and 34.92° of the lyocell fabric correspond to the crystal structures (1-10), (110), (020), and (004) plane of cellulose II (French. 2014). The spectra of the FR-lyocell are similar to that of the control sample, indicating the finishing process having no significant influence on the crystal structure of the lyocell fiber (Wan et al. 2019b).

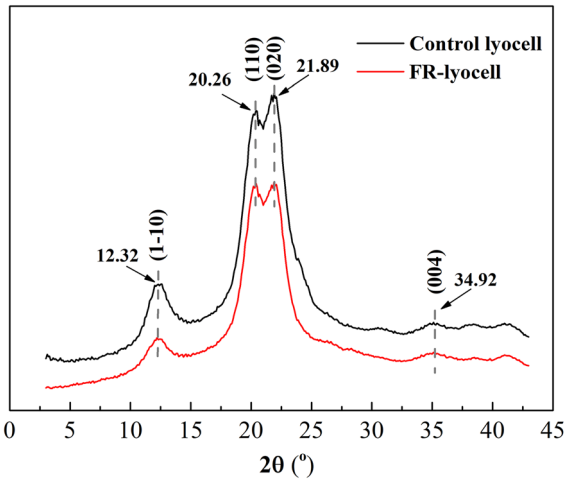

Fig. 5 XRD spectra of control lyocell and FR-lyocell

Thermal degradation analysis

The TGA and DTG curves of the control lyocell, FR-lyocell, and FR-lyocell (30 LCs) under nitrogen (a) and air (b) atmosphere are shown in Fig. 6. The detailed data are summarized in Table 3. As shown in Fig. 6a, the control lyocell began to decrease rapidly when the temperature reached 313.1 °C. In addition, the mass loss rate slowed down when the temperature reached 391.7 °C. Ultimately, approximately a 13.6 wt% char residue was retained at 800 °C. For the FR-lyocell, the temperature corresponding to 10 wt% weight loss ($T_{10\%}$) is at 222.2 °C, which is lower than that of the control lyocell. The mass of FR-lyocell rapidly decreased from 222.2 to 291.3 °C. Finally, 38.8 wt% char residue was obtained at 800 °C. The different char residue is due to the fact that FR contains numerous phosphorus and nitrogen components. As a result, lots of phosphoric acids, polyphosphoric acids, and other phosphorus-containing derivatives are evolved from phosphorus components during combustion, which facilitate the dehydration of cellulose to form more char residue (He et al. 2018). Meanwhile, non-combustible gases, such as ammonia (NH_3) generated by nitrogen components can dilute the concentration of flammable gases (Zhang and Shi 2019). In the case of FR-lyocell (30 LCs), the TGA curve is almost similar to that of FR-lyocell. The temperature corresponding to the maximum weight loss rate (T_{max}) is at 271.8 °C and the char residue at 800 °C is 37.1 wt%, which is slightly lower than that of FR-lyocell.

It can be seen from Fig. 6b, the weight loss tendency of all TGA curves is quite similar at low temperature (Li et al. 2020b). For control lyocell, the $T_{10\%}$ is at 288.8 °C and the main weight loss period ranges from 288.8 °C ($T_{10\%}$) to 367.4 °C (T_{max}) with a mass loss of about 67.8 wt%, which is mainly due to the release of aliphatic hydrocarbons or volatile products during pyrolysis process (Jiang et al. 2019). With temperature continually increasing, a new weight loss stage occurrs with about a 21.8 wt% mass loss, corresponding to the conversion of some aliphatic hydrocarbons to aromatic carbon and the production of CO and CO_2 during the carbonization of cellulose (Wang et al. 2018a, b). Finally, only 1.5 wt% char residue remains at 800 °C. For FR-lyocell, the $T_{10\%}$ is at 226.0 °C, which is much lower than that of control lyocell (288.8 °C). The treated lyocell exhibits

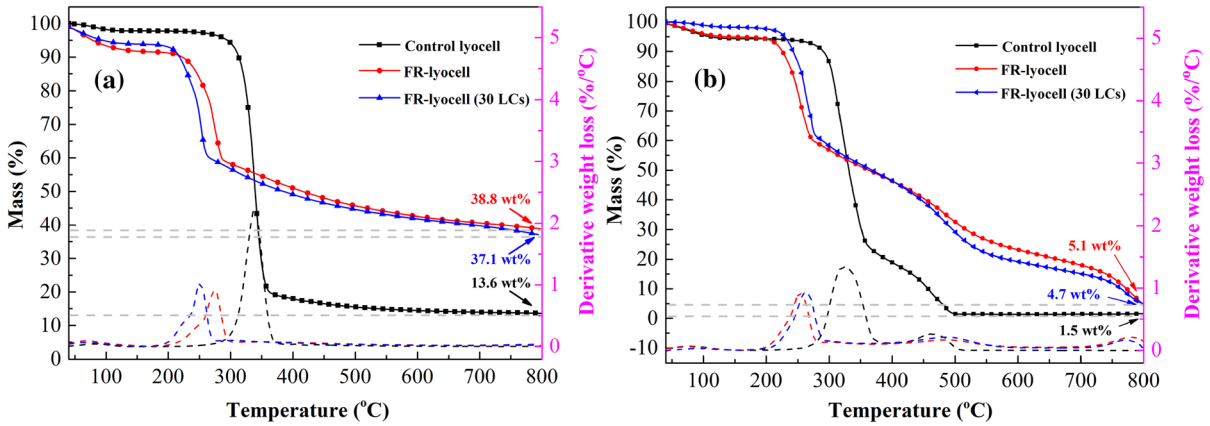

Fig. 6 TGA and DTG curves of control lyocell, FR-lyocell and FR-lyocell (30 LCs) in N_2 (**a**) and air (**b**) atmosphere

Table 3 TGA data of control lyocell, FR-lyocell and FR-lyocell (30 LCs) in N_2 and air atmosphere

Atmosphere	Sample	$T_{10\%}$ (°C)	T_{max} (°C)	Residue at 800 °C (wt%)
N_2	Control lyocell	313.1	391.7	13.6
	FR-lyocell	222.2	291.3	38.8
	FR-lyocell (30 LCs)	221.3	271.8	37.1
Air	Control lyocell	288.8	367.4	1.5
	FR-lyocell	226.0	286.7	5.1
	FR-lyocell (30 LCs)	244.5	285.1	4.7

a rapid decrease from 226.0 to 286.7 °C with about a 31.3 wt% mass loss. However, with the temperature increasing, there is a larger weight loss stage (Alongi et al. 2013). In this stage, the char residue begins to be furtherly oxidized and combustible volatiles (e.g. CO) and non-combustible volatiles (H_2O, NH_3, CO_2, etc.) are released. Ultimately, little char residue (5.1 wt%) at 800 °C is left. However, the amount of char residue of the modified lyocell is still higher than that of the pristine sample. The results fully prove that FR improves the thermal-oxidative stability and char-forming ability of lyocell fabrics. In the case of FR-lyocell (30 LCs), the TGA curve is basically similar to that of FR-lyocell. The T_{max} is at 285.1 °C and the char residue at 800 °C is about 4.7 wt%, which is slightly lower than that of FR-lyocell. These above phenomena can be explained that the P component of FR decomposes to form phosphoric acid and polyphosphoric acid, which can accelerate the degradation and promote the carbonization of lyocell fiber (Wan et al. 2019a). In addition, the N component of FR can generate non-combustible NH_3 to dilute the concentration of oxygen and flammable gases. In other words, the FR can play its flame retardant role both in condensed and gas phases. The above results indicate that FR-lyocell presents a higher thermostability and better flame retardancy than the control lyocell.

Cone calorimetry

The flame retardancy of the specimens was further evaluated by cone calorimetry. The HRR (a) and THR (b) curves of the control lyocell and FR-lyocell were presented in Fig. 7. Meanwhile, the corresponding data were listed in Table 4. As shown in Fig. 7a and Table 4, the control lyocell fabric was easily ignited with a time to ignition (TTI) of 18 s and reached the PHRR (144.7 kW/m^2) at 45 s. Ultimately, only 8.8 wt% of char residue was left. In contrast, for the FR-lyocell, it failed to ignite and delayed reaching the PHRR (12.4 kW/m^2) at 95 s. In addition, the THR of FR-lyocell was 2.1 MJ/m^2, which was much lower than that of the control lyocell (5.5 MJ/m^2). Finally, 12.3 wt% of char residue was remained, which was slightly higher than that of the control sample. Furthermore, the fire growth rate index (FIGRA) was

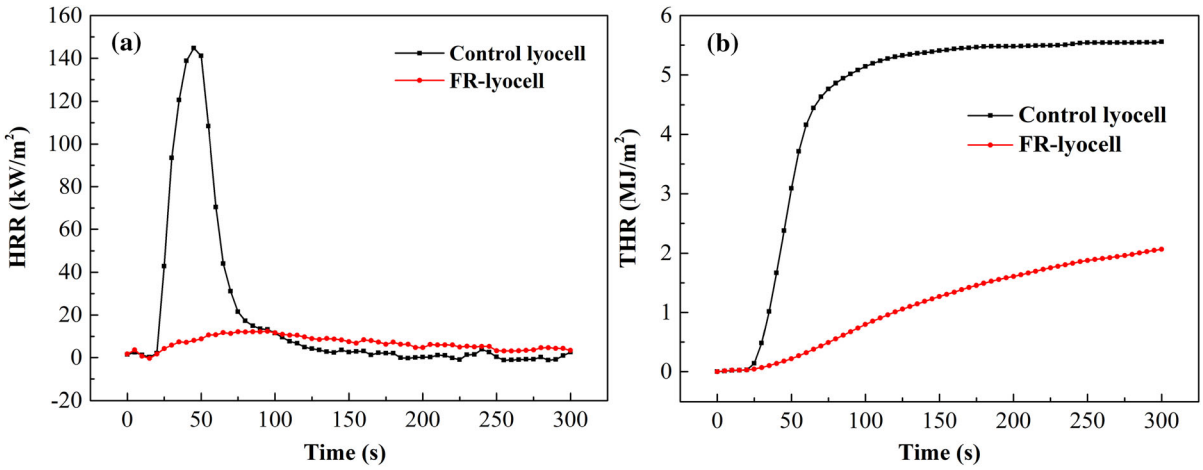

Fig. 7 HRR (**a**) and THR (**b**) curves of control lyocell and FR-lyocell fabrics

Table 4 Combustion parameters of control lyocell and FR-lyocell

Samples	TTI (s)	PHRR (kW/m^2)	T_{PHRR} (s)	Av-HRR (kW/m^2)	THR (MJ/m^2)	Residue (%)	FIGRA (kW/m^2 s)
Control lyocell	18.0 (± 1.0)	144.7 (± 5.0)	45.0 (± 1.0)	19.6 (± 1.0)	5.5 (± 0.4)	8.8 (± 0.8)	3.21 (± 0.26)
FR-lyocell	–	12.4 (± 0.9)	95.0 (± 1.6)	6.9 (± 0.6)	2.1 (± 0.3)	12.3 (± 0.6)	0.13 (± 0.04)

calculated by the ratio of PHRR to the time to PHRR (T_{PHRR}). It represents the fire growth rate and the scale of a fire (Ren et al. 2016, 2018). The FIGRA of FR-lyocell decreased from 3.21 to 0.13 kW/m^2 s. These results indicated that the phosphorus-rich and nitrogen-rich halogen-free flame retardant made lyocell fabrics have excellent flame retardancy.

TG-IR spectroscopy

To further explore the flame retardant mechanism of FR-lyocell fabrics, the TG-IR was used to detect the gaseous compounds produced during thermal decomposition of control lyocell and FR-lyocell under nitrogen atmosphere in real-time. The TG-IR spectra of the control lyocell and FR-lyocell at different temperatures are shown in Fig. 8. For the control lyocell (Fig. 8a), the peak at 3593 cm^{-1} is due to the stretching vibration absorption of O–H in H_2O (Alongi et al. 2011a; Wang et al. 2018a, b; Ding et al. 2017). The peaks at 2914 cm^{-1} and 2974 cm^{-1} are attributed to the vibration absorption of the C–H bond of the fabrics (Ren et al. 2016). The strong absorption peaks at 1744 cm^{-1} and 1060 cm^{-1} are assigned to the stretching vibration of C=O bonds from carbonyl compounds (Gaan and Sun 2007; Ren et al. 2020; Liu et al. 2018a, b) and C–O–C bond of ethers (Zhu and Shi 2003; Jia et al. 2017; Parsa and Chaffee 2018). The peaks at 2362 cm^{-1}, 2306 cm^{-1}, and 663 cm^{-1} are the stretching vibration absorption of CO_2 (Ji et al. 2018; Li et al 2020b). In addition, the faint peak at 2181 cm^{-1} is attributed to the stretching vibration absorption of CO. Therefore, the main degradation products of control lyocell include incombustible compounds (such as H_2O and CO_2) and flammable substances (such as hydrocarbons, carbonyls, and ethers). For the FR-lyocell (Fig. 8b), the strong absorption peak at 1526 cm^{-1} is assigned to the vibration absorption of the NH bond from the release of NH_3 (Echeverria et al. 2019; Wan et al. 2019b). The peaks at 2974 cm^{-1} and 1060 cm^{-1} are disappeared, implying the generation of combustible alkanes and ether being inhibited. Besides, the peak strength at 1744 cm^{-1} and 2363 cm^{-1} of the FR-lyocell fabrics is

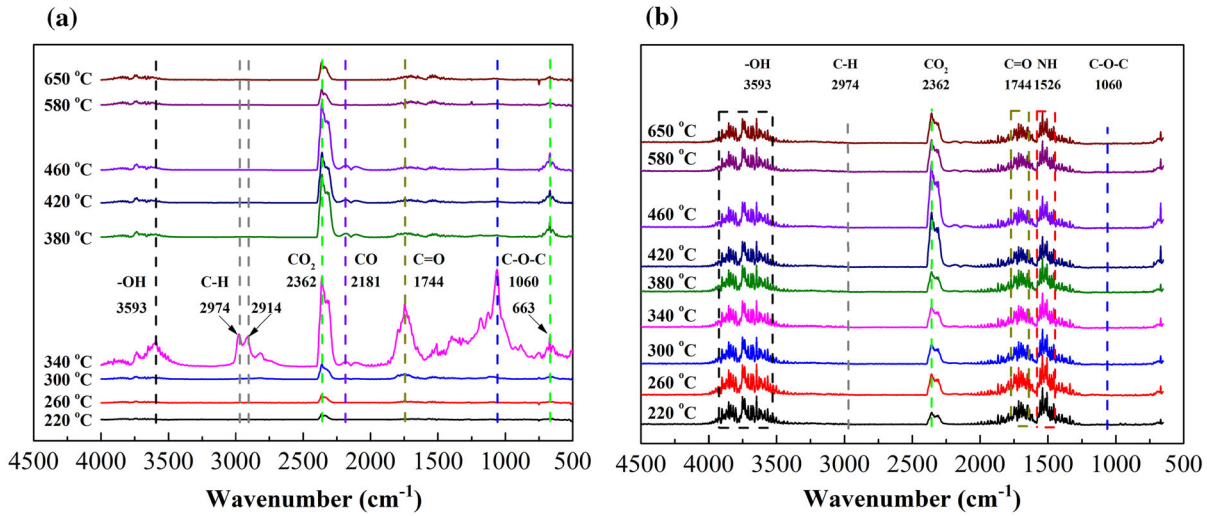

Fig. 8 TG-IR spectra of control lyocell fabric (**a**) and FR-lyocell fabric (**b**) at different temperatures

significantly lower than that of the pristine fabrics. The absorption intensities of H_2O at 3593 cm^{-1} are relatively stronger than that of pure lyocell. Consistent with the above description, the absorption peak of the treated lyocell (Fig. 8b) was simpler than that of control lyocell (Fig. 8a). These results indicate that FR is beneficial to dehydration and carbonization of fibers, resulting in forming more char residue instead of flammable substances (Wan et al. 2019b; Wang et al. 2016), which can prevent heat and fuel from the flame (Jia et al. 2017).

Raman spectroscopy analysis

To further understand the flame retardant mechanism, the char residue of FR-lyocell fabrics has been studied by Raman spectroscopy (Liu et al. 2017a; Peng et al. 2019). The Raman spectra of the FR-lyocell fabrics after combustion is shown in Fig. 9. It can be clearly seen that FR-lyocell exhibits two absorption peak bands at 1347 cm^{-1} and 1569 cm^{-1}, which are assigned to the D-band of graphite carbon and G-band of amorphous carbon, respectively (Chen and Wang 2009; Liu et al. 2018a, b). Specifically, the ratio of the integrated D and G bands intensities (I_D/I_G) can express the degree of graphitization of materials. Generally, the lower value of I_D/I_G means the microstructure of the char is better and has fewer defects. The I_D/I_G value of FR-lyocell is 0.771, indicating good graphitization degree of the char

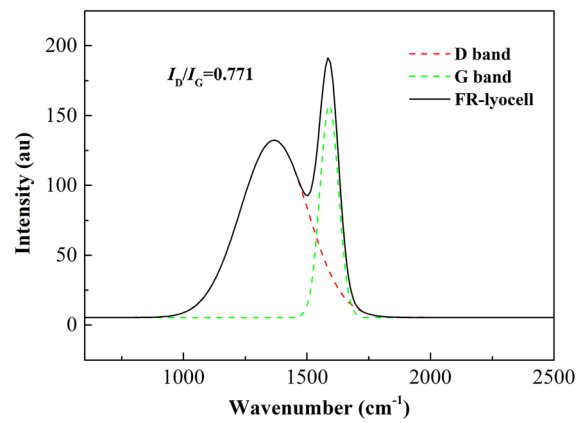

Fig. 9 Raman spectra of the char residue of FR-lyocell

residue and superior char formation capability. Therefore, the result confirms that FR can promote the formation of effective char residue on the surface of lyocell fabric to improve its flame retardance. (Duan et al. 2016).

Scanning electron microscopy-energy dispersive X-ray spectroscopy (SEM–EDS)

In order to examine the effect of flame retardant on microstructures of lyocell fabric, the surface morphology and elemental composition of the control lyocell, FR-lyocell, and the char residue of FR-lyocell fabric were detected by SEM–EDS. Figure 10a clearly shows that the control lyocell exhibits a smooth and

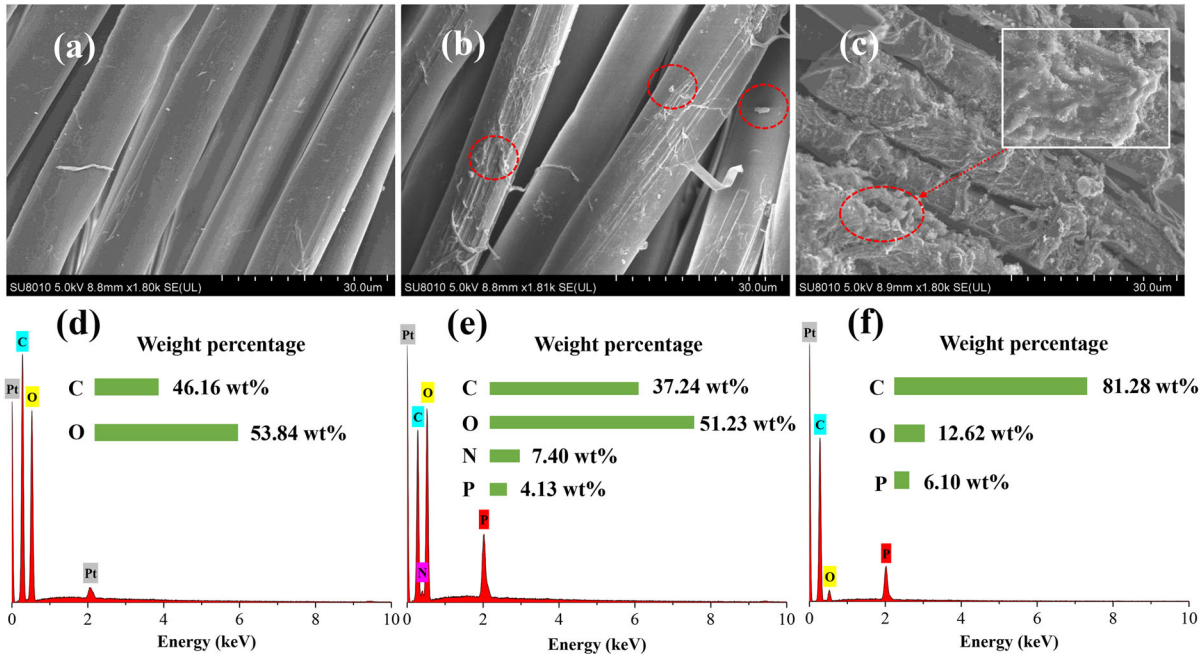

Fig. 10 SEM images and element content spectra of control lyocell fabric (**a**, **d**); FR-lyocell fabric (**b**, **e**) and the char residue of FR-lyocell fabric (**c**, **f**)

uniform surface. As illustrated in Fig. 10b, the surface structure of the FR-lyocell fabric has no obvious change compared with the control fabric. This is because FR has a low molecular weight and good water solubility. It can easily infiltrate into the interior of lyocell fiber and graft with cellulose (Jia et al. 2017; Lu et al. 2018a, b). For the char residue of FR-lyocell fabric (Fig. 10c), it is clearly observed that the char residue is dense and continuous. This phenomenon implies that FR can promote the formation of a complete char layer to hinder the combustion of the lyocell fabric. Meanwhile, there are no defects in the section, which indicates that the char layer has an effective condensed phase flame retardant effect.

For Fig. 10d, the elemental compositions and contents of control lyocell are mainly carbon (C) and oxygen (O), and the contents are 46.16 wt% and 53.84 wt%, respectively. Figure 10e exhibits the presence of C, O, N, and P elements. Especially, N and P contents of the FR-lyocell are 7.40 wt% and 4.13 wt%, respectively. From Fig. 10f, it can be observed that the N element disappears and the P content slightly increases (6.10 wt%). Furthermore, the C content significantly increases from 37.24 wt% of FR-lyocell to 81.28 wt% of the char residue. This is because N element generates NH_3 during combustion, at the same time, P element evolves into various phosphorus derivatives, facilitating the dehydration of cellulose to form more char residue (Zhang et al. 2020; Liu et al. 2017b). EDX analysis verified that the FR rich in phosphorus and nitrogen was grafted onto lyocell fiber by the strong P–O–C and N–C–P covalent bonds (Wan et al. 2019b).

Mechanical property

Figure 11 shows the tensile curves of lyocell and FR-lyocell fabrics. The corresponding tensile results are summarized in Table 5. It can be seen from Table 5 and Fig. 11 that the tensile strength of control lyocell fabric is 15.51 MPa, with an elongation at break of 13.67%. Moreover, the tensile strength of lyocell fabric treated with 20 wt%, 30 wt% and 40 wt% FR finishing solution is 15.07 MPa, 14.83 MPa and 13.00 MPa, respectively. The result indicates that with flame retardant concentration increasing, the tensile strength of FR-lyocell fabric slightly reduces. It may be due to the fact that the grafting reaction between FR and the hydroxyl groups (–OH) of cellulose weakens the interaction of intermolecular

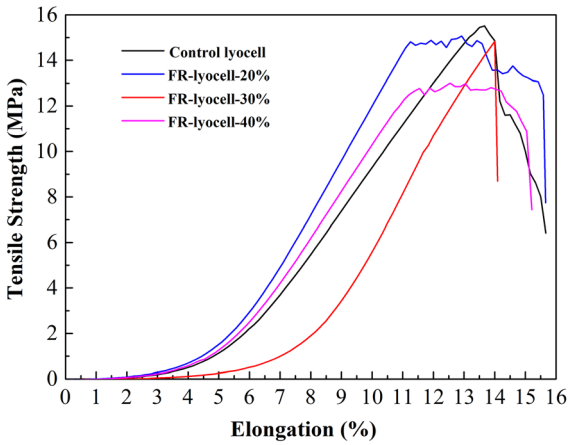

Fig. 11 Tensile curves of control lyocell and FR-lyocell fabrics treated by different FR concentrations

hydrogen bonds. However, the elongation at break of lyocell fabric treated with 20 wt%, 30 wt% and 40 wt% FR finishing solution is 14.00%, 12.92% and 12.54%, respectively. This indicates that lyocell fabrics treated by FR have negligible impact on elongation at break. The above results illustrates that the tensile strength of lyocell fabrics treated by FR is slightly reduced but has an insignificant impact on its applications in the textile field.

Flame retardant mechanism

Based on the above analysis, the flame retardancy mechanism is proposed in Fig. 12. Upon heating, the phosphorus-containing moiety in the FR will be decomposed to form numerous PO· free radicals, which can capture the gas phase free radicals produced by the decomposition of cellulose molecules, such as H· and ·OH, thus interrupting the degradation process initiated by cellulose chain free radicals. On the other hand, phosphorus-containing acids, for example, phosphoric acid, pyrophosphoric acid or polyphosphoric acid species can be produced, which can facilitate cellulose dehydration to generate more carbonaceous substances (He et al. 2018; Zhang et al. 2020; Liu et al. 2017b). As a result, the carbonaceous layer can isolate the heat transfer and the diffusion of small combustible products created by the degradation of cellulose and oxygen. Meanwhile, non-combustible gases (such as NH_3) are generated by nitrogen components in FR when it is burning. In addition, the FR contains C and O components, which can release lots of water vapor and CO_2 during the combustion process. Therefore, the incombustible gases (NH_3, H_2O, and CO_2) can dilute the concentration of O_2 and flammable gases in the combustion zone, thus slowing down the combustion and decreasing the heat release rate. In summary, the FR plays a dual flame retardant effect in the gaseous and condensed phase.

Conclusions

A novel effective halogen-free flame retardant (FR) rich in phosphorus (P) and nitrogen (N) was synthesized via Mannich and esterification reaction and used for preparation of durable flame retardant lyocell (FR-lyocell). NMR, FTIR, and XPS indicated that the FR was successfully synthesized and grafted on the surface of the lyocell fabric via firm P–O–C covalent bonds. The results obtained from ICP and EA confirmed that the FR was rich P and N contents. Additionally, XRD analysis indicated that the finishing process had no significant influence on the crystal structure of the lyocell fiber. The LOI data

Table 5 Mechanical properties of control lyocell and FR-treated lyocell fabric

Samples	Tensile strength (MPa)	Elongation at break (%)
Control lyocell	15.51 (± 0.57)	13.67 (± 0.12)
FR-lyocell-20%	15.07 (± 0.35)	14.00 (± 0.20)
FR-lyocell-30%	14.83 (± 0.46)	12.92 (± 0.17)
FR-lyocell-40%	13.00 (± 0.66)	12.54 (± 0.15)

Lyocell fabric treated with 20 wt%, 30 wt% and 40 wt% FR finishing solution is denoted as FR-lyocell-20%, FR-lyocell-30% and FR-lyocell-40%

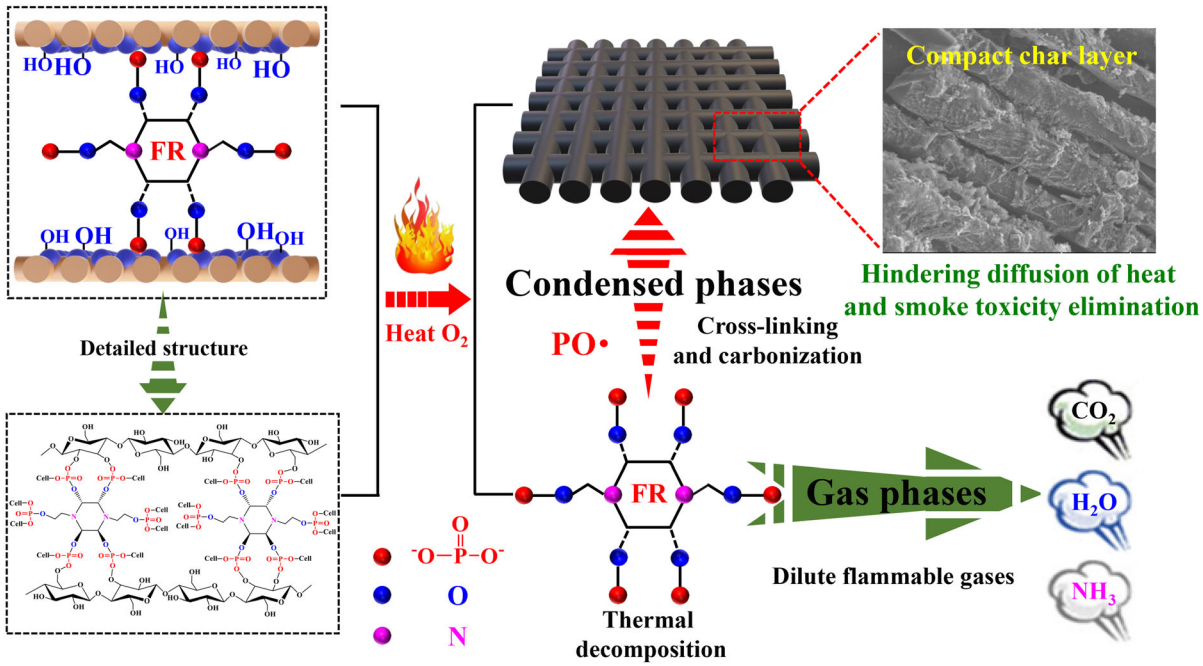

Fig. 12 Possible flame-retardant mechanism of FR for lyocell fabric

demonstrated that FR-lyocell possessed outstanding flame retardancy. TGA and SEM results exhibited that FR-lyocell degraded preferentially and was prone to form more continuous and compact char residue. Raman spectra confirmed that FR-lyocell had a superior char forming capability. In addition, cone calorimeter test revealed that FR-lyocell had lower PHRR and THRR than that of control lyocell and could not be ignited. Furthermore, TG-IR results demonstrated that volatile products were significantly reduced and numerous inflammable gases, such as NH_3, CO_2 were generated during the combustion of FR-lyocell. The tensile strength of lyocell fabrics treated by FR was slightly reduced. The above results revealed that the FR-lyocell exhibited excellent flame retardancy, superior char forming capability.

Acknowledgments The authors are very grateful to the financial supports of the National Natural Science Foundation of China (No. 51573134) and the National Key Research and Development Program of China (2017YFB0309000).

Authors' contribution YBG and MYX contributed equally to this work. YBG conceived the idea and designed the experiments. MYX contributed to the material fabrication. YBG conducted the thermal properties measurement and analyzed the corresponding results. MYX was responsible for the SEM images, the combustion testing, FT-IR measurements. YBG and MYX contributed to the cone calorimeter test and the corresponding analysis. YLR and XHL co-wrote and revised the manuscript. All authors commented on the final manuscript.

Declarations

Conflict of interest The authors declare that they have no known competing financial interests or personal relationships that could have appeared to influence the work reported in this paper. All the authors listed have approved the manuscript enclosed.

Ethical statement All authors state that they adhere to the Ethical Responsibilities of Authors. In addition, the work is compliance with ethical standards.

References

Alongi J, Ciobanu M, Malucelli G (2011a) Novel flame retardant finishing systems for cotton fabrics based on phosphorus-containing compounds and silica derived from sol–gel processes. Carbohyd Polym 85:599–608. https://doi.org/10.1016/j.carbpol.2011.03.024

Alongi J, Tata J, Frache A (2011b) Hydrotalcite and nanometric silica as finishing additives to enhance the thermal stability and flame retardancy of cotton. Cellulose 18:179–190. https://doi.org/10.1007/s10570-010-9473-z

Alongi J, Carletto RA, Di Blasio A, Carosio F, Bosco F, Malucelli G (2013) DNA: a novel, green, natural flame

retardant and suppressant for cotton. J Mater Chem A 1(15):36–40. https://doi.org/10.1039/c3ta00107e

Bai BC, Kim EA, Jeon YP, Lee CW, In SJ, Lee YS, Im JS (2014) Improved flame retardant properties of lyocell fiber achieved by phosphorus compound. Mater Lett 135:226–228. https://doi.org/10.1016/j.matlet.2014.07.131

Chen L, Wang YZ (2009) A review on flame retardant technology in China. Part I: development of flame retardants. Polym Adv Technol 21:1–26. https://doi.org/10.1002/pat.1550

Chen XL, Huo LL, Jiao CM, Li SX (2013) TG-FTIR characterization of volatile compounds from flame retardant polyurethane foams materials. J Anal Appl Pyrol 100:186–191. https://doi.org/10.1016/j.jaap.2012.12.017

Cheng YY, He G, Barras A, Coffinier Y, Lu SX, Xu WG, Szunerits S, Boukherroub R (2017) One-step immersion for fabrication of superhydrophobic/superoleophilic carbon felts with fire resistance: fast separation and removal of oil from water. Chem Eng J 331:372–382. https://doi.org/10.1016/j.cej.2017.08.088

Ding HY, Huang K, Li SH, Xu LN, Xia JL, Li M (2017) Synthesis of a novel phosphorus and nitrogen-containing bio-based polyol and its application in flame retardant polyurethane foam. J Anal Appl Pyrol 128:102–113. https://doi.org/10.1016/j.jaap.2017.10.020

Dong CH, He PS, Lu Z, Wang SG, Sui SY, Liu J, Zhang L, Zhu P (2017) Preparation and properties of cotton fabrics treated with a novel antimicrobial and flame retardant containing triazine and phosphorus components. J Therm Anal Calorim 87(11):1–9. https://doi.org/10.1007/s10973-017-6604-x

Duan LJ, Yang HY, Song L, Hou YB, Wang W, Gui Z, Hu Y (2016) Hyperbranched phosphorus/nitrogen-containing polymer in combination with ammonium polyphosphate as a novel flame retardant system for polypropylene. Polym Degrad Stab 134:179–185. https://doi.org/10.1016/j.polymdegradstab.2016.10.004

Echeverria CA, Handoko W, Pahlevani F, Sahajwalla V (2019) Cascading use of textile waste for the advancement of fibre reinforced composites for building applications. J Clean Prod 208:1524–1536. https://doi.org/10.1016/j.jclepro.2018.10.227

Feng YJ, Zhou Y, Li DK, He SA, Zhang FX, Zhang GX (2017) A plant-based reactive ammonium phytate for use as a flame retardant for cotton fabric. Carbohydr Polym 175:636–644. https://doi.org/10.1016/j.carbpol.2017.06.129

French AD (2014) Idealized powder diffraction patterns for cellulose polymorphs. Cellulose 21:885–896. https://doi.org/10.1007/s10570-013-0030-4

Gaan S, Sun G (2007) Effect of phosphorus and nitrogen on flame retardant cellulose: a study of phosphorus compounds. J Anal Appl Pyrolysis 78:371–377. https://doi.org/10.1016/j.jaap.2006.09.010

Gao WW, Zhang GX, Zhang FX (2015) Enhancement of flame retardancy of cotton fabrics by grafting a novel organic phosphorous-based flame retardant. Cellulose 22:2787–2796. https://doi.org/10.1007/s10570-015-0641-z

Grancaric AM, Botteri L, Alongi J, Malucelli G (2015) Synergistic effects occurring between water glasses and urea/ammonium dihydrogen phosphate pair for enhancing the flame retardancy of cotton. Cellulose 22:2825–2835. https://doi.org/10.1007/s10570-015-0671-6

He PS, Chen XY, Zhu P, Liu J, Fan GD, Sui SY, Lu Z, Dong CH (2018) Preparation and flame retardancy of reactive flame retardant for cotton fabric. J Therm Anal Calorim 132:1771–1781. https://doi.org/10.1007/s10973-018-7057-6

Ji YM, Chen GQ, Xing TL (2018) Rational design and preparation of flame retardant silk fabrics coated with reduced graphene oxide. Appl Surf Sci 474:203–210. https://doi.org/10.1016/j.apsusc.2018.03.120

Jia YL, Lu Y, Zhang GX, Liang YJ, Zhang FX (2017) Facile synthesis of an eco-friendly nitrogen-phosphorus ammonium salt to enhance durability and flame retardancy of cotton. J Mater Chem A 5:9970–9981. https://doi.org/10.1039/C7TA01106G

Jiang ZM, Li H, He YW, Liu Y, Dong CH, Zhu P (2019) Flame retardancy and thermal behavior of cotton fabrics based on a novel phosphorus-containing siloxane. Appl Surf Sci 479:765–775. https://doi.org/10.1016/j.apsusc.2019.02.159

Joshi HD, Joshi DH, Patel MG (2010) Dyeing and finishing of lyocell union fabrics: an industrial study. Color Technol 126:194–200. https://doi.org/10.1111/j.1478-4408.2010.00248.x

Kazantsev OA, Arifullin IR, Savinova MV, Sivokhin AP, Bol'shakova YA, Shchegravina ES (2020) Two-stage one-pot synthesis of N-(dibutylaminomethyl)-methacrylamide by Mannich reaction in mild conditions with high yield. React Chem Eng 5(9):1791–1797. https://doi.org/10.1039/x0xx00000x

Li YC, Schulz J, Mannen S, Delhom C, Condon B, Chang S, Zammarano M, Grunlan JC (2010) Flame retardant behavior of polyelectrolyte-clay thin film assemblies on cotton fabric. ACS Nano 4:3325–3337. https://doi.org/10.1021/nn100467e

Li P, Liu C, Xu YJ, Jiang ZM, Liu Y, Zhu P (2020a) Novel and eco-friendly flame-retardant cotton fabrics with lignosulfonate and chitosan through LbL: flame retardancy, smoke suppression and flame-retardant mechanism. Polym Degrad Stab 181:109302. https://doi.org/10.1016/j.polymdegradstab.2020.109302

Li P, Wang B, Liu YY, Xu YJ, Jiang ZM, Dong CH, Zhang L, Liu Y, Zhu P (2020b) Fully bio-based coating from chitosan and phytate for fire-safety and antibacterial cotton fabrics. Carbohyd Polym 237:116173. https://doi.org/10.1016/j.carbpol.2020.116173

Liang TY, Jiang ZL, Wang CS, Liu JL (2017) A facile one-step synthesis of flame retardant coatings on cotton fabric via ultrasound irradiation. J Appl Polym Sci 134(30):45114–45120. https://doi.org/10.1002/app.45114

Liu XH, Zhang QY, Cheng BW, Ren YL, Zhang YG, Ding C (2017a) Durable flame retardant cellulosic fibers modified with novel, facile and efficient phytic acid-based finishing agent. Cellulose 25:799–811. https://doi.org/10.1007/s10570-017-1550-0

Liu ZY, Xu MJ, Wang Q, Li B (2017b) A novel durable flame retardant cotton fabric produced by surface chemical

grafting of phosphorus- and nitrogen-containing compounds. Cellulose 24:4069–4081. https://doi.org/10.1007/s10570-017-1391-x

Liu XH, Zhang YG, Cheng BW, Ren YL, Zhang QY, Ding C, Peng B (2018a) Preparation of durable and flame retardant lyocell fibers by a one-pot chemical treatment. Cellulose 25:6745–6758. https://doi.org/10.1007/s10570-018-2005-y

Liu Y, Wang QQ, Jiang ZM, Zhang CJ, Li ZF, Chen HQ, Zhu P (2018b) Effect of chitosan on the fire retardancy and thermal degradation properties of coated cotton fabrics with sodium phytate and APTES by LBL assembly. J Anal Appl Pyrolysis 135:289–298. https://doi.org/10.1016/j.jaap.2018.08.024

Liu MS, Huang S, Zhang GX, Zhang FX (2019) An efficient anti-flaming phosphorus-containing guanazole derivative for cotton fabric. Cellulose 26(4):2791–2804. https://doi.org/10.1007/s10570-019-02275-6

Liu XH, Ding C, Peng B, Ren YL, Cheng BW, Lin SG, He J, Su XW (2020) Synthesis and application of a new, facile, and efficient sorbitol-based finishing agent for durable and flame retardant lyocell fibers. Cellulose 27(6):3427–3442. https://doi.org/10.1007/s10570-019-02894-z

Lu Y, Jia YL, Zhang GX, Zhang FX (2018a) An eco-friendly intumescent flame retardant with high efficiency and durability for cotton fabric. Cellulose 25:5389–5404. https://doi.org/10.1007/s10570-018-1930-0

Lu Y, Jia YL, Zhou Y, Zou J, Zhang GX, Zhang FX (2018b) Straightforward one-step solvent-free synthesis of the flame retardant for cotton with excellent efficiency and durability. Carbohydr Polym 201:438–455. https://doi.org/10.1016/j.carbpol.2018.08.078

Mengal N, Syed U, Malik SA, Sahito IA, Jeong SH (2016) Citric acid based durable and sustainable flame retardant treatment for lyocell fabric. Carbohydr Polym 153:78–88. https://doi.org/10.1016/j.carbpol.2016.07.074

Naik AD, Fontaine G, Bellayer S, Bourbigot S (2015) Salen based Schiff bases to flame retard thermoplastic polyurethane mimicking operational strategies of thermosetting resin. RSC Adv 5:48224–48235. https://doi.org/10.1039/c5ra06242j

Parsa MR, Chaffee AL (2018) The effect of densification with NaOH on brown coal thermal oxidation behaviour and structure. Fuel 216:548–558. https://doi.org/10.1016/j.fuel.2017.11.135

Peng HY, Wang D, Li M, Zhang LP, Liu MM, Fu SH (2019) Ultra-small SiO_2 nanospheres selt-pollinated on flowerlike MoS_2 for simultaneously reinforcing mechanical, thermal and flame retardant properties of polyacrylonitrile fiber. Compos Part B-Eng 174:107037. https://doi.org/10.1016/j.compositesb.2019.107037

Peng Y, Niu M, Qin RH, Xue BX, Shao MQ (2020) Study on flame retardancy and smoke suppression of PET by the synergy between Fe_2O_3 and new phosphorus-containing silicone flame retardant. High Perform Polym 32(8):871–882. https://doi.org/10.1177/0954008320914365

Ren YL, Zhang Y, Zhao JY, Wang XL, Zeng Q, Gu YT (2016) Phosphorus-doped organic-inorganic hybrid silicon coating for improving fire retardancy of polyacrylonitrile fabric. J Sol-Gel Sci Technol 82:280–288. https://doi.org/10.1007/s10971-016-4273-z

Ren YL, Huo TG, Qin YW, Liu XH (2018) Preparation of flame retardant polyacrylonitrile fabric based on sol–gel and layer-by-layer assembly. Materials 11:483. https://doi.org/10.3390/ma11040483

Ren YL, Liu YS, Wang Y, Guo X, Liu XH (2020) Preparation of durable and flame retardant lyocell fabrics by using a biomass-based modifier derived from vitamin C. Cellulose 27(11):6677–6689. https://doi.org/10.1007/s10570-020-03218-2

Sahito IA, Sun KC, Arbab AA, Qadir MB, Jeong SH (2015) Integrating high electrical conductivity and photocatalytic activity in cotton fabric by cationizing for enriched coating of negatively charged graphene oxide. Carbohydr Polym 130:299–306. https://doi.org/10.1016/j.carbpol.2015.05.010

Seddon H, Hall M, Horrocks AR (1996) The flame retardancy of lyocell fibres. Polym Degrad Stab 54:401–402. https://doi.org/10.1016/s0141-3910(96)00070-5

Shibata M, Oyamada S, Kobayashi S, Yaginuma D (2004) Mechanical properties and biodegradability of green composites based on biodegradable polyesters and lyocell fabric. J Appl Polym Sci 92:3857–3863. https://doi.org/10.1002/app.20405

Tian PX, Liu MS, Wan CY, Zhang GX, Zhang FX (2019) Synthesis of a formaldehyde-free flame retardant for cotton fabric. Cellulose 26(18):9889–9899. https://doi.org/10.1007/s10570-019-02751-z

Wan CY, Liu MS, Tian PX, Zhang GX, Zhang FX (2019a) Renewable vitamin B5 reactive N–P flame retardant endows cotton with excellent fire resistance and durability. Cellulose 27(3):1745–1761. https://doi.org/10.1007/s10570-019-02886-z

Wan CY, Tian PX, Liu MS, Zhang GX, Zhang FX (2019b) Synthesis of a phosphorus–nitrogen flame retardant endowing cotton with high whiteness and washability. Ind Crops Prod 141:111738. https://doi.org/10.1016/j.indcrop.2019.111738

Wang LH, Ren YL, Wang XL, Zhao JY, Zhang Y, Zeng Q, Gu YT (2016) Fire retardant viscose fiber fabric produced by graft polymerization of phosphorus and nitrogen-containing monomer. Cellulose 23:2689–2700. https://doi.org/10.1007/s10570-016-0970-6

Wang DF, Zhong L, Zhang C, Li SN, Tian PX, Zhang FX, Zhang GX (2018a) Ecofriendly synthesis of a highly efficient phosphorus flame retardant based on xylitol and application on cotton fabric. Cellulose 26:2123–2138. https://doi.org/10.1007/s10570-018-2193-5

Wang Z, Shu X, Zhu H, Xie L, Cheng S, Zhang Y (2018b) Characteristics of biochars prepared by co-pyrolysis of sewage sludge and cotton stalk intended for use as soil amendments. Environ Technol 41(11):1347–1357. https://doi.org/10.1080/09593330.2018.1534891

Wang B, Xu YJ, Li P, Zhang FQ, Liu Y, Li P (2020) Flame-retardant polyester/cotton blend with phosphorus/nitrogen/silicon-containing nano-coating by layer-by-layer assembly. Appl Surf Sci 509:145323. https://doi.org/10.1016/j.apsusc.2020.145323

Wei DD, Dong CH, Chen ZH, Liu J, Li Q, Lu Z (2018) A novel cyclic copolymer containing Si/P/N used as flame retardant

and water repellent agent on cotton fabrics. J Appl Polym Sci. https://doi.org/10.1002/app.47280

Xie KL, Gao AQ, Zhang YS (2013) Flame retardant finishing of cotton fabric based on synergistic compounds containing boron and nitrogen. Carbohydr Polym 98:706–710. https://doi.org/10.1016/j.carbpol.2013.06.014

Xu L, Jiang Y, Qiu R (2017) Parametric study and global sensitivity analysis for co-pyrolysis of rape straw and waste tire via variance-based decomposition. Bioresour Technol 247:545–552. https://doi.org/10.1016/j.biortech.2017.09.141

Xu F, Zhong L, Xu Y, Feng SY, Zhang C, Zhang FX, Zhang GX (2018) Highly efficient flame retardant kraft paper. Polymers 54:1884–1897. https://doi.org/10.1007/s10853-018-2911-2

Yang TT, Guan JP, Tang RC, Chen GQ (2018) Condensed tannin from *Dioscorea cirrhosa* tuber as an eco-friendly and durable flame retardant for silk textile. Ind Crops Prod 115:16–25. https://doi.org/10.1016/j.indcrop.2018.02.018

Zhang XS, Shi MW (2019) Flame retardant vinylon/poly(m-phenylene isophthalamide) blended fibers with synergistic flame retardancy for advanced fireproof textiles. J Hazard Mater 365:9–15. https://doi.org/10.1016/j.jhazmat.2018.10.091

Zhang QY, Liu XH, Ren YL, Zhang YG, Cheng BW (2020) Fabrication of a high phosphorus-nitrogen content modifier with star structure for effectively enhancing flame retardancy of lyocell fibers. Cellulose 27(14):8369–8383. https://doi.org/10.1007/s10570-020-03333-0

Zhu SW, Shi WF (2003) Thermal degradation of a new flame retardant phosphate methacrylate polymer. Polym Degrad Stab 80:217–222. https://doi.org/10.1016/S0141-3910(02)00401-9